

## 2. RECIPROCAL SPACE IN CRYSTAL-STRUCTURE DETERMINATION

patterns]. Contact J. M. Zuo or J. C. H. Spence, Physics Department, Arizona State University, Tempe, Arizona, USA.

(2) A package for CBED pattern simulation by both Bloch-wave and multi-slice methods is available from P. Stadelmann (pierre.stadelmann@cime.uhd.edfl.ch), Lausanne, Switzerland, in UNIX for workstations [Silicon Graphics, Dec Alpha (OSF), IBM RISC 6000, SUN and HP-9000].

(3) HOLZ line simulations: Listing for PC 8801 (NEC): Tanaka & Terauchi (1985, pp. 174–175).

### 2.5.4. Electron-diffraction structure analysis (EDSA)

(B. K. VAINSHTEIN AND B. B. ZVYAGIN)

#### 2.5.4.1. Introduction

Electron-diffraction structure analysis (EDSA) (Vainshtein, 1964) based on electron diffraction (Pinsker, 1953) is used for the investigation of the atomic structure of matter together with X-ray and neutron diffraction analysis. The peculiarities of EDSA, as compared with X-ray structure analysis, are defined by a strong interaction of electrons with the substance and by a short wavelength  $\lambda$ . According to the Schrödinger equation (see Section 5.2.2) the electrons are scattered by the electrostatic field of an object. The values of the atomic scattering amplitudes,  $f_e$ , are three orders higher than those of X-rays,  $f_x$ , and neutrons,  $f_n$ . Therefore, a very small quantity of a substance is sufficient to obtain a diffraction pattern. EDSA is used for the investigation of very thin single-crystal films, of  $\sim 5$ – $50$  nm polycrystalline and textured films, and of deposits of finely grained materials and surface layers of bulk specimens. The structures of many ionic crystals, crystal hydrates and hydro-oxides, various inorganic, organic, semiconducting and metallo-organic compounds, of various minerals, especially layer silicates, and of biological structures have been investigated by means of EDSA; it has also been used in the study of polymers, amorphous solids and liquids.

Special areas of EDSA application are: determination of unit cells; establishing orientational and other geometrical relationships between related crystalline phases; phase analysis on the basis of  $d_{hkl}$  and  $I_{hkl}$  sets; analysis of the distribution of crystallite dimensions in a specimen and inner strains in crystallites as determined from line profiles; investigation of the surface structure of single crystals; structure analysis of crystals, including atomic position determination; precise determination of lattice potential distribution and chemical bonds between atoms; and investigation of crystals of biological origin in combination with electron microscopy (Vainshtein, 1964; Pinsker, 1953; Zvyagin, 1967; Pinsker *et al.*, 1981; Dorset, 1976; Zvyagin *et al.*, 1979).

There are different kinds of electron diffraction (ED) depending on the experimental conditions: high-energy (HEED) (above 30–200 kV), low-energy (LEED) (10–600 V), transmission (THEED), and reflection (RHEED). In electron-diffraction studies use is made of special apparatus – electron-diffraction cameras in which the lens system located between the electron source and the specimen forms the primary electron beam, and the diffracted beams reach the detector without aberration distortions. In this case, high-resolution electron diffraction (HRED) is obtained. ED patterns may also be observed in electron microscopes by a selected-area method (SAD). Other types of electron diffraction are: MBD (microbeam), HDD (high-dispersion), CBD (convergent-beam), SMBD (scanning-beam) and RMBD (rocking-beam) diffraction (see Sections 2.5.2 and 2.5.3). The recent development of electron diffractometry, based on direct intensity registration and measurement by scanning the diffraction pattern against a fixed detector (scintillator followed by photomultiplier), presents a new improved level of EDSA which

provides higher precision and reliability of structural data (Avilov *et al.*, 1999; Tsipursky & Drits, 1977; Zhukhlistov *et al.*, 1997, 1998; Zvyagin *et al.*, 1996).

Electron-diffraction studies of the structure of molecules in vapours and gases is a large special field of research (Vilkov *et al.*, 1978). See also *Stereochemical Applications of Gas-Phase Electron Diffraction* (1988).

#### 2.5.4.2. The geometry of ED patterns

In HEED, the electron wavelength  $\lambda$  is about  $0.05 \text{ \AA}$  or less. The Ewald sphere with radius  $\lambda^{-1}$  has a very small curvature and is approximated by a plane. The ED patterns are, therefore, considered as plane cross sections of the reciprocal lattice (RL) passing normal to the incident beam through the point 000, to scale  $L\lambda$  (Fig. 2.5.4.1). The basic formula is

$$r = |\mathbf{h}|L\lambda, \text{ or } rd = L\lambda, \quad (2.5.4.1)$$

where  $r$  is the distance from the pattern centre to the reflection,  $\mathbf{h}$  is the reciprocal-space vector,  $d$  is the appropriate interplanar distance and  $L$  is the specimen-to-screen distance. The deviation of the Ewald sphere from a plane at distance  $h$  from the origin of the coordinates is  $\delta_h = h^2\lambda/2$ . Owing to the small values of  $\lambda$  and to the rapid decrease of  $f_e$  depending on  $(\sin \theta)/\lambda$ , the diffracted beams are concentrated in a small angular interval ( $\leq 0.1$  rad).

*Single-crystal ED patterns* image one plane of the RL. They can be obtained from thin ideal crystalline plates, mosaic single-crystal films, or, in the RHEED case, from the faces of bulk single crystals. Point ED patterns can be obtained more easily owing to the following factors: the small size of the crystals (increase in the dimension of RL nodes) and mosaicity – the small spread of crystallite orientations in a specimen (tangential tension of the RL nodes). The crystal system, the parameters of the unit cell and the Laue symmetry are determined from point ED patterns; the probable space group is found from extinctions. Point ED patterns may be used for intensity measurements if the kinematic approximation holds true or if the contributions of the dynamic and secondary scattering are not too large.

The indexing of reflections and the unit-cell determination are carried out according to the formulae relating the RL to the DL (direct lattice) (Vainshtein, 1964; Pinsker, 1953; Zvyagin, 1967).

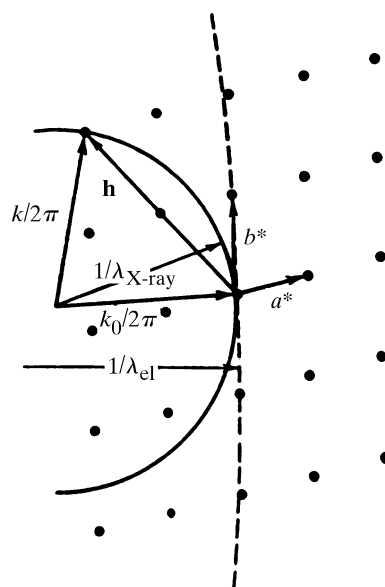


Fig. 2.5.4.1. Ewald spheres in reciprocal space. Dotted line: electrons, solid line: X-rays.

## 2.5. ELECTRON DIFFRACTION AND ELECTRON MICROSCOPY IN STRUCTURE DETERMINATION

Under electron-diffraction conditions crystals usually show a tendency to lie down on the substrate plane on the most developed face. Let us take this as (001). The vectors  $a$  and  $b$  are then parallel, while vector  $c^*$  is normal to this plane, and the RL points are considered as being disposed along direct lines parallel to the axis  $c^*$  with constant  $hk$  and variable  $l$ .

The interpretation of the point patterns as respective RL planes is quite simple in the case of orthogonal lattices. If the lattice is triclinic or monoclinic the pattern of the crystal in the position with the face (001) normal to the incident beam does not have to contain  $hk0$  reflections with non-zero  $h$  and  $k$  because, in general, the planes  $ab$  and  $a^*b^*$  do not coincide. However, the intersection traces of direct lines  $hk$  with the plane normal to them (plane  $ab$ ) always form a net with periods

$$(a \sin \gamma)^{-1}, (b \sin \gamma)^{-1}, \text{ and angle } \gamma' = \pi - \gamma \quad (2.5.4.2a)$$

(Fig. 2.5.4.2). The points  $hkl$  along these directions  $hk$  are at distances

$$\eta = ha^* \cos \beta^* + kb^* \cos \alpha^* + lc^* \quad (2.5.4.3)$$

from the  $ab$  plane.

By changing the crystal orientation it is possible to obtain an image of the  $a^*b^*$  plane containing  $hk0$  reflections, or of other RL planes, with the exception of planes making a small angle with the axis  $c^*$ .

In the general case of an arbitrary crystal orientation, the pattern is considered as a plane section of the system of directions  $hk$  which makes an angle  $\varphi$  with the plane  $ab$ , intersecting it along a direction  $[uv]$ . It is described by two periods along directions  $0h, 0k$ ;

$$(a \sin \gamma \cos \psi_h)^{-1}, (b \sin \gamma \cos \psi_k)^{-1}, \quad (2.5.4.2b)$$

with an angle  $\gamma''$  between them satisfying the relation

$$\cos \gamma'' = \sin \psi_h \sin \psi_k - \cos \psi_h \cos \psi_k \cos \gamma, \quad (2.5.4.2c)$$

and by a system of parallel directions

$$p_h h + p_k k = l; \quad l = 0, \pm 1, \pm 2, \dots \quad (2.5.4.4)$$

The angles  $\psi_h, \psi_k$  are formed by directions  $0h, 0k$  in the plane of the pattern with the plane  $ab$ . The coefficients  $p_h, p_k$  depend on the unit-cell parameters, angle  $\varphi$  and direction  $[uv]$ . These relations are used for the indexing of reflections revealed near the integer positions  $hkl$  in the pattern and for unit-cell calculations (Vainshtein, 1964; Zvyagin, 1967; Zvyagin *et al.*, 1979).

In RED patterns obtained with an incident beam nearly parallel to the plane  $ab$  one can reveal all the RL planes passing through  $c^*$  which become normal to the beam at different azimuthal orientations of the crystal.

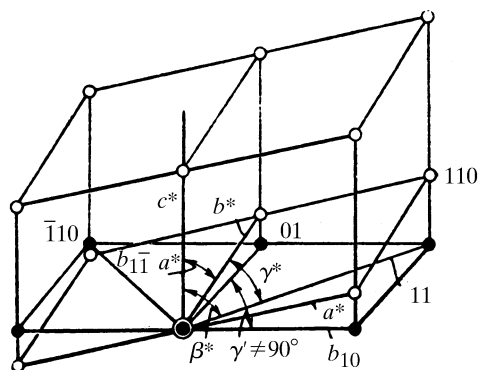


Fig. 2.5.4.2. Triclinic reciprocal lattice. Points: open circles, projection net; black circles.

With the increase of the thickness of crystals (see below, Chapter 5.1) the scattering becomes dynamical and Kikuchi lines and bands appear. Kikuchi ED patterns are used for the estimation of the degree of perfection of the structure of the surface layers of single crystals for specimen orientation in HREM (IT C, 1999, Section 4.3.8). Patterns obtained with a convergent beam contain Kossel lines and are used for determining the symmetry of objects under investigation (see Section 5.1.2).

*Texture ED patterns* are a widely used kind of ED pattern (Pinsker, 1953; Vainshtein, 1964; Zvyagin, 1967). Textured specimens are prepared by substance precipitation on the substrate, from solutions and suspensions, or from gas phase in vacuum. The microcrystals are found to be oriented with a common (developed) face parallel to the substrate, but they have random azimuthal orientations. Correspondingly, the RL also takes random azimuthal orientations, having  $c^*$  as the common axis, *i.e.* it is a rotational body of the point RL of a single crystal. Thus, the ED patterns from textures bear a resemblance, from the viewpoint of their geometry, to X-ray rotation patterns, but they are less complicated, since they represent a plane cross section of reciprocal space.

If the crystallites are oriented by the plane  $(hkl)$ , then the axis  $[hkl]^*$  is the texture axis. For the sake of simplicity, let us assume that the basic plane is the plane (001) containing the axes  $a$  and  $b$ , so that the texture axis is  $[001]^*$ , *i.e.* the axis  $c^*$ . The matrices of appropriate transformations will define a transition to the general case (see IT A, 1995). The RL directions  $hk = \text{constant}$ , parallel to the texture axis, transform to cylindrical surfaces, the points with  $\eta_{hkl} = \text{constant}$  are in planes perpendicular to the texture axis, while any 'tilted' lines transform to cones or hyperboloids of rotation. Each point  $hkl$  transforms to a ring lying on these surfaces. In practice, owing to a certain spread of  $c^*$  axes of single crystals, the rings are blurred into small band sections of a spherical surface with the centre at the point 000; the oblique cross section of such bands produces reflections in the form of arcs. The main interference curves for texture patterns are ellipses imaging oblique plane cross sections of the cylinders  $hk$  (Fig. 2.5.4.3).

At the normal electron-beam incidence (tilting angle  $\varphi = 0^\circ$ ) the ED pattern represents a cross section of cylinders perpendicular to the axis  $c^*$ , *i.e.* a system of rings.

On tilting the specimen to an angle  $\varphi$  with respect to its normal position (usually  $\varphi \simeq 60^\circ$ ) the patterns image an oblique cross section of the cylindrical RL, and are called oblique-texture (OT)

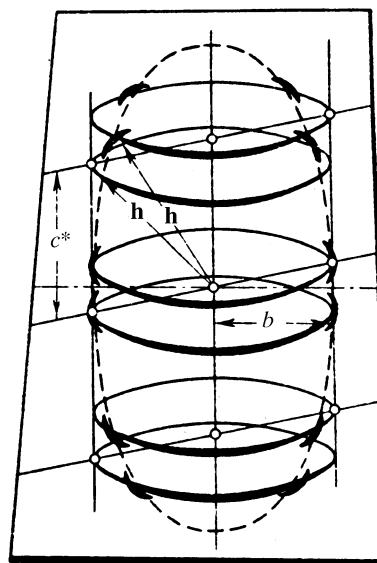


Fig. 2.5.4.3. Formation of ellipses on an electron-diffraction pattern from an oblique texture.

## 2. RECIPROCAL SPACE IN CRYSTAL-STRUCTURE DETERMINATION

ED patterns. The ellipses ( $hk = \text{constant}$ ) and layer lines ( $l = \text{constant}$ ) for orthogonal lattices are the main characteristic lines of ED patterns along which the reflections are arranged. The shortcoming of oblique-texture ED patterns is the absence of reflections lying inside the cone formed by rotation of the straight line coming from the point 000 at an angle  $(90^\circ - \varphi)$  around the axis  $c^*$  and, in particular, of reflections 00 $l$ . However, at  $\varphi \lesssim 60\text{--}70^\circ$  the set of reflections is usually sufficient for structural determination.

For unit-cell determination and reflection indexing the values  $d$  (i.e.  $|\mathbf{h}|$ ) are used, and the reflection positions defined by the ellipses  $hk$  to which they belong and the values  $\eta$  are considered. The periods  $a^*, b^*$  are obtained directly from  $h_{100}$  and  $h_{010}$  values. The period  $c^*$ , if it is normal to the plane  $a^*b^*$  ( $\gamma^*$  being arbitrary), is calculated as

$$c^* = \eta/l = (h_{hkl}^2 - h_{hk0}^2)^{1/2}/l. \quad (2.5.4.5a)$$

For oblique-angled lattices

$$c^* = [(h_{l+l}^2 + h_{l-l}^2 - 2h_l^2)/2]^{1/2}/l. \quad (2.5.4.5b)$$

In the general case of oblique-angled lattices the coaxial cylinders  $hk$  have radii

$$b_{hk} = (1/\sin \gamma)[(h^2/a^2) + (k^2/b^2) - (2hk \cos \gamma/ab)]^{1/2} \quad (2.5.4.6)$$

and it is always possible to use the measured or calculated values  $b_{hk}$  in (2.5.4.5a) instead of  $h_{hk0}$ , since

$$\eta = (h_{hkl}^2 - b_{hk}^2)^{1/2}. \quad (2.5.4.7)$$

In OT patterns the  $b_{hk}$  and  $\eta$  values are represented by the lengths of the small axes of the ellipses  $B_{hk} = L\lambda b_{hk}$  and the distances of the reflections  $hkl$  from the line of small axes (equatorial line of the pattern)

$$D_{hkl} = L\lambda\eta/\sin \varphi = hp + ks + lq. \quad (2.5.4.8)$$

Analysis of the  $B_{hk}$  values gives  $a, b, \gamma$ , while  $p, s$  and  $q$  are calculated from the  $D_{hkl}$  values. It is essential that the components of the normal projections  $c_n$  of the axis  $c$  on the plane  $ab$  measured in the units of  $a$  and  $b$  are

$$\begin{aligned} x_n &= (c/a)(\cos \beta - \cos \alpha \cos \gamma)/\sin^2 \gamma \\ &= -p/q, \\ y_n &= (c/b)(\cos \alpha - \cos \beta \cos \gamma)/\sin^2 \gamma \\ &= -s/q. \end{aligned} \quad (2.5.4.9)$$

Obtaining  $x_n, y_n$  one can calculate

$$c_n = [(x_n a)^2 + (y_n b)^2 + 2x_n y_n ab \cos \gamma]^{1/2}.$$

Since

$$\begin{aligned} d_{001} &= L\lambda/q \sin \varphi, \\ c &= (c_n^2 + d_{001}^2)^{1/2}. \end{aligned} \quad (2.5.4.10)$$

The  $\alpha, \beta$  values are then defined by the relations

$$\begin{aligned} \cos \alpha &= (x_n a \cos \gamma + y_n b)/c, \\ \cos \beta &= (x_n a + y_n b \cos \gamma)/c. \end{aligned} \quad (2.5.4.11)$$

Because of the small particle dimensions in textured specimens, the kinematic approximation is more reliable for OT patterns, enabling a more precise calculation of the structure amplitudes from the intensities of reflections.

*Polycrystal ED patterns.* In this case, the RL is a set of concentric spheres with radii  $h_{hkl}$ . The ED pattern, like an X-ray powder pattern, is a set of rings with radii

$$r_{hkl} = h_{hkl}L\lambda. \quad (2.5.4.12)$$

### 2.5.4.3. Intensities of diffraction beams

The intensities of scattering by a crystal are determined by the scattering amplitudes of atoms in the crystal, given by (see also Section 5.2.1)

$$\begin{aligned} f_e^{\text{abs}}(s) &= 4\pi K \int \varphi(r)r^2 \frac{\sin sr}{sr} dr, \\ K &= \frac{2\pi me}{h^2}; f_e = K^{-1}f_e^{\text{abs}}, \end{aligned} \quad (2.5.4.13)$$

where  $\varphi(r)$  is the potential of an atom and  $s = 4\pi(\sin \theta)/\lambda$ . The absolute values of  $f_e^{\text{abs}}$  have the dimensionality of length  $L$ . In EDSA it is convenient to use  $f_e$  without  $K$ . The dimensionality of  $f_e$  is [potential  $L^3$ ]. With the expression of  $f_e$  in  $\text{V \AA}^3$  the value  $K^{-1}$  in (2.5.4.13) is  $47.87 \text{ V \AA}^2$ .

The scattering atomic amplitudes  $f_e(s)$  differ from the respective  $f_x(s)$  X-ray values in the following: while  $f_x(0) = Z$  (electron shell charge), the atomic amplitude at  $s = 0$

$$f_e(0) = 4\pi \int \varphi(r)r^2 dr \quad (2.5.4.14)$$

is the 'full potential' of the atom. On average,  $f_e(0) \simeq Z^{1/3}$ , but for small atomic numbers  $Z$ , owing to the peculiarities in the filling of the electron shells,  $f_e(0)$  exhibits within periods of the periodic table of elements 'reverse motion', i.e. they decrease with  $Z$  increasing (Vainshtein, 1952, 1964). At large  $(\sin \theta)/\lambda$ ,  $f_e \simeq Z$ . The atomic amplitudes and, consequently, the reflection intensities, are recorded, in practice, up to values of  $(\sin \theta)/\lambda \simeq 0.8\text{--}1.2 \text{ \AA}^{-1}$ , i.e. up to  $d_{\text{min}} \simeq 0.4\text{--}0.6 \text{ \AA}$ .

The structure amplitude  $\Phi_{hkl}$  of a crystal is determined by the Fourier integral of the unit-cell potential (see Chapter 1.2),

$$\Phi_{hkl} = \int_{\Omega} \varphi(\mathbf{r}) \exp\{2\pi i(\mathbf{r} \cdot \mathbf{h})\} d\mathbf{r}, \quad (2.5.4.15)$$

where  $\Omega$  is the unit-cell volume. The potential of the unit cell can be expressed by the potentials of the atoms of which it is composed:

$$\varphi(\mathbf{r}) = \sum_{\text{cell}, i} \varphi_{\text{at } i}(\mathbf{r} - \mathbf{r}_i). \quad (2.5.4.16)$$

The thermal motion of atoms in a crystal is taken into account by the convolution of the potential of an atom at rest with the probability function  $w(\mathbf{r})$  describing the thermal motion:

$$\varphi_{\text{at}} = \varphi_{\text{at}}(\mathbf{r}) * w(\mathbf{r}). \quad (2.5.4.17)$$

Accordingly, the atomic temperature factor of the atom in a crystal is

$$f_{eT}[(\sin \theta)/\lambda] = f_e f_T = f_e [(\sin \theta)/\lambda] \exp\{-B[(\sin \theta)/\lambda]^2\}, \quad (2.5.4.18)$$

where the Debye temperature factor is written for the case of isotropic thermal vibrations. Consequently, the structure amplitude is

$$\Phi_{hkl} = \sum_{\text{cell}, i} f_{eT,i} \exp\{2\pi i(hx_i + ky_i + lz_i)\}. \quad (2.5.4.19)$$

This general expression is transformed (see IT I, 1952) according to the space group of a given crystal.

To determine the structure amplitudes in EDSA experimentally, one has to use specimens satisfying the kinematic scattering condition, i.e. those consisting of extremely thin crystallites. The